

Mean-Lifetime Measurements within the Superdeformed Second Minimum in ^{132}Ce

A. J. Kirwan, G. C. Ball,^(a) P. J. Bishop, M. J. Godfrey, P. J. Nolan, and D. J. Thornley
Oliver Lodge Laboratory, University of Liverpool, Liverpool L69 3BX, United Kingdom

and

D. J. G. Love and A. H. Nelson
Daresbury Laboratory, Daresbury, Warrington WA4 4AD, United Kingdom
 (Received 15 September 1986)

A rotational band has been studied in ^{132}Ce to a spin above $50\hbar$. Lifetime measurements have resulted in a large quadrupole moment corresponding to a deformation $\beta \sim 0.5$. This is consistent with the moment of inertia determined from the energy-level spacing. These data are the first measurements of collectivity of discrete lines at high spin within the superdeformed second minimum.

PACS numbers: 23.20.Ck, 21.10.Re, 27.60.+j

Nuclei are known to contain states with a much higher deformation than that seen in ground states. These superdeformed structures have been of considerable interest for many years.¹ One of the best known examples is fission isomers.^{2,3} Evidence was found for superdeformation at high spin in ^{152}Dy ⁴ from γ - γ energy correlations within the continuum. The first experimental indication of a superdeformed structure that decayed by discrete-line gamma transitions was found in ^{132}Ce .⁵ A sequence of states was observed to beyond spin $40\hbar$, whereas the ground-state sequence was only seen to spin $30\hbar$. Some spectacular data have recently been published⁶ on ^{152}Dy showing a superdeformed band also de-

caying by discrete gamma transitions, but now to spin $60\hbar$. In both cases the moment of inertia was used to determine the deformation giving, assuming a rigid body, $\beta \sim 0.45$ (^{132}Ce) and $\beta \sim 0.6$ (^{152}Dy). The determination of transition strengths is a much more reliable way of deducing the deformation. Such measurements were attempted on continuum data in ^{152}Dy , but only resulted in limits.⁷ In this Letter we report measurements of mean lifetimes for the states in ^{132}Ce . The measurements confirm superdeformation and extend the band beyond $50\hbar$.

The experiments were carried out at Daresbury Laboratory using the TESSA3 spectrometer. This is similar

TABLE I. Gamma-ray energies, relative intensities, and mean lifetimes.

| E_γ (keV) | I^π | Relative intensity ^a | Observed F^b | Apparent τ (fs) ^c | τ (fs) ^d |
|---------------------|---------|------------------------------------|-------------------|--------------------------------------|--------------------------|
| 809 | 20 | 85(10) | 0.50(3) | 435(50) | 85(30) |
| 865 | 22 | 100(7) | 0.62(1) | 280(12) | 90(20) |
| 929 | 24 | 110(12) | 0.74(2) | 170(15) | 40(17) |
| 995 | 26 | 103(13) | 0.80(2) | 125(15) | <25 |
| 1060 | 28 | 105(9) | 0.82(1) | 108(8) | <30 |
| 1127 | 30 | 91(3) | 0.85(1) | 88(7) | 20(10) |
| 1195 | 32 | 94(7) | 0.89(1) | 62(6) | 14(11) |
| 1264 | 34 | 84(3) | 0.91(1) | 50(6) | <20 |
| 1335 | 36 | 62(11) | 0.93(1) | 37(6) | <10 |
| 1409 | 38 | 51(9) | 0.93(1) | 37(6) | <15 |
| 1488 | 40 | 29(7) | 0.94(2) | 32(11) | <15 |
| 1567 | 42 | 39(3) | 0.94(2) | 32(11) | <35 |
| 1652 | 44 | 46(5) | 0.99(2) | <15 | <10 |
| 1742 | 46 | 21(7) | 0.98(3) | <25 | |
| 1836 | 48 | 25(10) | | | |
| 1930 | 50 | | | | |
| 2030 | 52 | | | | |

^aNormalized to 865 keV=100, equivalent to 5% of the $4^+ - 2^+$ intensity in ^{132}Ce .

^bThe attenuated Doppler shift F is the ratio of the average velocity at which each state decays to the initial recoil velocity.

^cNo feeding correction.

^dCorrected for feeding.

to TESSA2,⁸ but has twelve bismuth germanate (BGO) suppressed germanium detectors⁹ in addition to the 50-element BGO array. Three experiments were performed, all using the reaction $^{100}\text{Mo}(^{36}\text{S},4n)^{132}\text{Ce}$. In each case the BGO array was used to select gamma rays in ^{132}Ce and events were recorded corresponding to two or more coincident suppressed detectors. The first used a $1\text{-mg}\cdot\text{cm}^{-2}$ ^{100}Mg target on a gold backing (15 mg cm^{-2}) at a beam energy of 150 MeV; approximately 2×10^8 events were recorded and mean lifetimes deduced using the Doppler-shift-attenuation method.¹⁰ The other experiments employed thin ^{100}Mo targets to look for states at higher spin. Over 3×10^8 events were recorded at beam energies of 150 and 160 MeV.

The data have allowed the band to be extended beyond $50\hbar$; the transition energies are given in Table I. Previously we showed that this band decays into the yrast sequence at spins 16 and 18; the linking transitions were not identified. There was no indication in the new high-statistics data of discrete linking transitions below 3 MeV. In what follows it is assumed that $2\hbar$ are removed by the unseen linking transitions and that the decays in the band are stretched $E2$'s. The data are compared to the results of a theoretical calculation¹¹ in Fig. 1. The band lies $(4-6)\hbar$ higher in the calculations and the lines

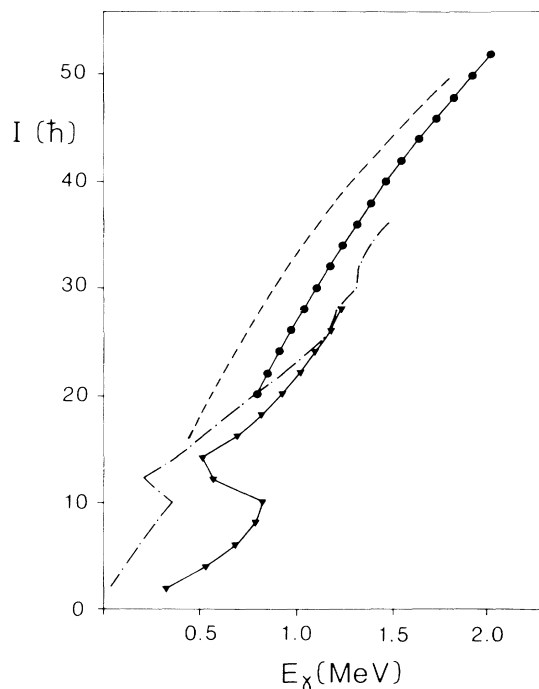


FIG. 1. Spin (I) vs gamma-ray energy (E_γ) for two bands in ^{132}Ce . The experimental data are for the yrast band (triangles) and the superdeformed band (circles). Their calculated counterparts are also shown (pairing not included), yrast band (dot-dashed line) and superdeformed band (dashed line).

are curved even though a constant deformation is predicted. The relative intensities of gamma rays in the band are given in Table I. The relatively strong population (5% of the 4^+-2^+ transition) of such high-spin states allows further spectroscopic measurements to be made. The highest transition seen in the band has an energy above 2 MeV, corresponding to one of the highest rotational frequencies ($>1\text{ MeV}/\hbar$) at which discrete lines have been studied in heavy nuclei.

The thin- and backed-target data are shown in Figs. 2(a) and 2(b). The spectra clearly show wide peaks below 1150 keV for the backed target indicating measurable lifetimes. The transitions from higher-spin states are the same in both spectra indicating short lifetimes. Standard techniques¹⁰ using a centroid shift analysis gave the results in Table I and Fig. 3. The average recoil velocity ($\langle v/c\cos\theta \rangle$) at which each state decays was determined from the data taken at 35° and 145° and is independent of the unshifted transition energy. The data were also used to determine the attenuation factor F (Table I), a calculated initial recoil velocity being used to determine the full Doppler shift. The smoothness of the data points (Fig. 3) as a function of spin indicates no significant slow side feeding into the band at high spin; the observed line shapes also show no slow component.

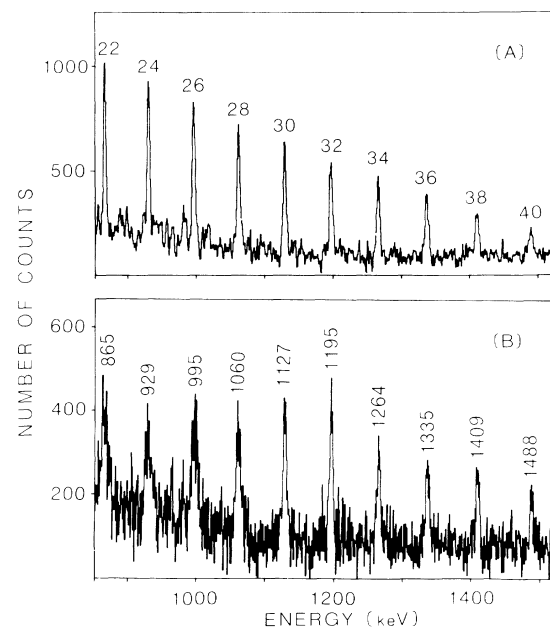


FIG. 2. Partial gamma-ray spectra from the reaction $^{100}\text{Mo}(^{36}\text{S},4n)^{132}\text{Ce}$. The data are a sum over all detector angles ($35^\circ, 90^\circ, 145^\circ$), the gains being matched assuming a full Doppler shift. The spectra are the sum of several gates in the superdeformed band. (a) Thin target, labeled by spins; (b) backed target, labeled by gamma-ray energies.

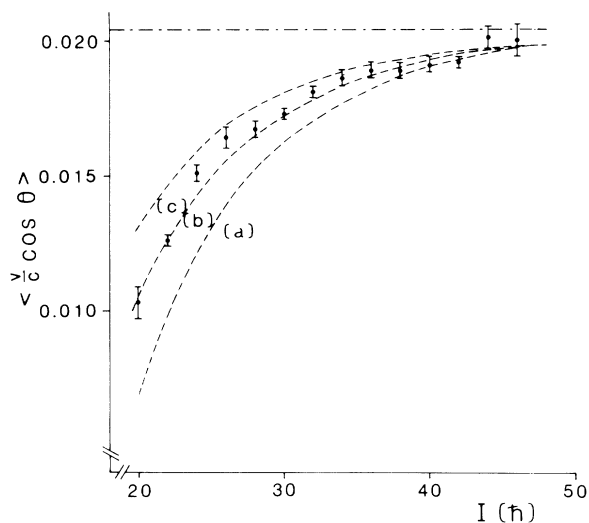


FIG. 3. The average recoil velocity for the decay of each state in the superdeformed band, obtained using a centroid shift analysis at angles of 35° and 145° . The expected curves (dashed line) for a rotational band with a constant deformation are shown normalized to the average of the four transitions at high spin [(40–46) \hbar]. Curve *b* corresponds to a quadrupole moment $Q_0 = 8.8 e \cdot b$ ($\beta \sim 0.5$). Curves *a* and *c* correspond to a change in Q_0 of $\pm 20\%$. Also shown is the kinematically calculated initial recoil velocity (dot-dashed line).

The conversion of the centroid shift to mean lifetime requires a knowledge of the slowing down of the recoils in the target and its backing. The electronic stopping powers used were those from Northcliffe and Schilling¹² normalized to the α -particle stopping powers of Ziegler and Chu.¹³ The nuclear stopping powers used were those of Lindhard, Scharff, and Schiott,¹⁴ with scattering included using the method given by Blaugrund.¹⁵ This analysis method is known to be satisfactory for a centroid shift analysis.¹⁰ As the slowest recoil velocity found in the data was $v/c \sim 1\%$ the results are relatively insensitive to the nuclear stopping.

In Fig. 3, three curves are shown. These assume decay within a single rotational band of constant deformation fed 100% at high spin. The average population time for each state is calculated within the rotational model. The stopping power is then used to convert this to an average recoil velocity. The curves are normalized to the average of the four transitions at high spin [(40–46) \hbar]. The data are consistent with the assumption of a single band with quadrupole moment $Q_0 = 8.8 e \cdot b$ ($\beta \sim 0.5$).¹⁶ The data also imply that the feeding into the band between 34 \hbar and 50 \hbar is from states with comparable lifetimes. Lifetimes are also deduced for individual levels. The apparent mean lifetime (Table I) is deduced directly from the F factor with no correction for feeding. This is the average time at which each state decays. The actual

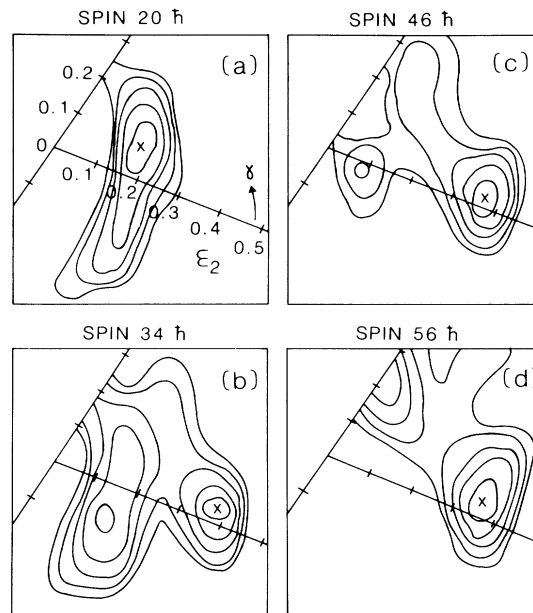


FIG. 4. Potential-energy surfaces in the ϵ_2 vs γ plane for ^{132}Ce (Lund convention for γ) (Ref. 17) carried out using a method similar to Ref. 11 with a value of $\epsilon_4 = \epsilon_2/6$. The minimum in the potential is shown by a cross; contours are at 0.2-MeV intervals. (a) 20 \hbar , (b) 34 \hbar , (c) 46 \hbar , and (d) 56 \hbar .

mean lifetimes in the final column are deduced by correcting for 100% cascade feeding. This assumption is valid for states with spin $\leq 32\hbar$ (see relative intensities in Table I) and should be a good approximation for higher states as the discussion above suggests that side feeding times are comparable to the cascade feeding times. In Fig. 3, the calculated initial recoil velocity is shown. The difference between this value and the high-spin data points corresponds to a feeding time into these states of 10–15 fs.

These states correspond to those predicted in the second minima in the potential. Figure 4 shows potential energy surfaces for ^{132}Ce in the spin range (20–56) \hbar . A minimum appears near $\epsilon_2 \sim 0.38$ ($\beta \sim 0.45$) which becomes yrast near 30 \hbar ; however, above 50 \hbar an oblate minimum starts to develop. The highest spin we see in the band is $\sim 50\hbar$, which does not increase between 150 and 160 MeV even though $\sim 8\hbar$ more spin is taken into the compound nucleus.

In conclusion, we have observed a rotational band in ^{132}Ce to above spin 50 \hbar . Lifetimes measured for these states show that they are members of a superdeformed band. These data are the first measurements of collectivity from discrete gamma transitions at high spin within the second minimum. The strong population of states within the second minimum with $\sim 5\%$ of the ^{132}Ce cross section (i.e., ~ 10 mb) opens a new and ex-

citing era.

This work was supported by grants from the United Kingdom Science and Engineering Research Council. We are grateful to the Lund University group for the use of their potential-energy-surface code. We acknowledge the receipt of a Science and Engineering Research Council Visiting Fellowship (G.C.B.) and Science and Engineering Research Council postgraduate studentships (P.J.B., M.J.G., and D.J.T.).

^(a)Permanent address: Chalk River Nuclear Laboratories, Atomic Energy of Canada Limited, Chalk River, Ontario, Canada K0J 1J0.

¹T. Bengtsson, M. E. Faber, G. Leander, P. Möller, M. Ploszajczak, I. Ragnarsson, and S. Åberg, *Phys. Scr.* **24**, 200 (1981).

²S. M. Polikanov *et al.*, *Zh. Eksp. Teor. Fiz.* **42**, 1464 (1962) [*Sov. Phys. JETP* **15**, 1016 (1962)].

³H. J. Specht, J. Weber, E. Konecny, and D. Heunemann, *Phys. Lett.* **41B**, 43 (1972).

⁴B. M. Nyakó *et al.*, *Phys. Rev. Lett.* **52**, 507 (1984).

⁵P. J. Nolan, A. J. Kirwan, D. J. G. Love, A. H. Nelson, D. J. Unwin, and P. J. Twin, *J. Phys. G* **11**, L17 (1985).

⁶P. J. Twin *et al.*, *Phys. Rev. Lett.* **57**, 811 (1986).

⁷P. J. Twin *et al.*, *Phys. Rev. Lett.* **55**, 1380 (1985).

⁸P. J. Twin, P. J. Nolan, R. Aryaeinejad, D. J. G. Love, A. H. Nelson, and A. J. Kirwan, *Nucl. Phys.* **A409**, 343c (1983).

⁹P. J. Nolan, D. W. Gifford, and P. J. Twin, *Nucl. Instrum. Methods Phys. Res., Sect. A* **236**, 95 (1985).

¹⁰P. J. Nolan and J. F. Sharpey-Schafer, *Rep. Prog. Phys.* **42**, 1 (1979).

¹¹T. Bengtsson and I. Ragnarsson, *Nucl. Phys.* **A436**, 14 (1985), and private communication.

¹²L. C. Northcliffe and R. F. Schilling, *Nucl. Data Tables A* **7**, 233 (1970).

¹³J. F. Ziegler and W. K. Chu, *At. Data Nucl. Data Tables* **13**, 463 (1974).

¹⁴J. Lindhard, M. Scharff, and H. E. Schiott, *K. Dan. Vidensk. Selsk., Mat.-Fys. Medd.* **33**, No. 14 (1963).

¹⁵A. E. Blaugrund, *Nucl. Phys.* **88**, 501 (1966).

¹⁶K. E. G. Lobner, M. Vetter, and V. Hönl, *Nucl. Data Tables A* **7**, 495 (1970).

¹⁷S. Frauendorf and F. R. May, *Phys. Lett.* **125B**, 245 (1983).